Community Structure in a Soil Porous System

Juan Pablo Cárdenas, Antonio Santiago, Ana María Tarquis, Juan Carlos Losada, Florentino Borondo, and Rosa M. Benito

Abstract: Soil is well recognized as a highly complex system. The interaction and coupled physical, chemical, and biological processes and phenomena occurring in the soil environment at different spatial and temporal scales are the main reasons for such complexity. There is a need for appropriate methodologies to characterize soil porous systems with an interdisciplinary character.

Four different real soil samples, presenting different textures, have been modeled as heterogeneous complex networks, applying a model known as the heterogeneous preferential attachment. An analytical study of the degree distributions in the soil model shows a multiscaling behavior in the connectivity degrees, leaving an empirically testable signature of heterogeneity in the topology of soil pore networks. We also show that the power-law scaling in the degree distribution is a robust trait of the soil model.

Last, the detection of spatial pore communities, as densely connected groups with only sparser connections between them, has been studied for the first time in these soil networks. Our results show that the presence of these communities depends on the parameter values used to construct the network. These findings could contribute to understanding the mechanisms of the diffusion phenomena in soils, such as gas and water diffusion, development and dynamics of microorganisms, among others.

Key words: Porous soil model, community structure, networks.

Diffusion controls the gaseous transport process through porous medium when advective transport is almost null. Knowledge of the soil structure and pore connectivity are critical issues to understand and model soil aeration, sequestration or emission of greenhouse gases, and volatilization of volatile organic chemicals (Ball et al., 2007). Even more, in any transport process in soils, it is a requirement to study soil structure and pore connectivity to extract as much information as possible, applying different methodologies. In the last decades, these issues have gained notoriety as scientists have realized that soil is one of the most complex materials on Earth, within which many biological, physical, and chemical processes that support life and affect climate change take place.

A quantitative and explicit characterization of the porous media of soils is difficult because of the complexity of the pore space (Leij et al., 2002; VandenBygaart et al., 1999). This is the main reason why most theoretical approaches to soil porosity are idealizations to simplify the complex structure of the connections and spatial location of pores (Bird et al., 2006; Tarquis et al., 2009). Considering this problem, several works have tried to achieve a more realistic view of the structure of porous media, taking into account the complex relation between pores (Cárdenas et al., 2010; Mooney and Korošak, 2009; Santiago et al., 2008). In an attempt to capture the complexity of the system, we developed a model, the porous soil model, which incorporates the differing pore properties as well as their interaction patterns. In this model, we interpret porous soils as heterogeneous networks where pores are abstracted as nodes, characterized by their size and spatial location, and the links representing connections between them. The networks of pores are generated by a model known as the heterogeneous preferential attachment (HPA) (Santiago and Benito, 2007a, 2007b, 2008, 2009), a generalization of the Barabási-Albert model (Barabási and Albert, 1999) to heterogeneous networks. Developing an exhaustive analysis of the model, we obtained analytical solutions for the degree densities and degree distribution of the pore networks generated by the model approaching the limit of highest number of nodes (thermodynamic limit) and have shown that the networks can exhibit similar properties to those observed in other complex networks (Santiago and Benito, 2007a).

We studied the topological properties of these soil networks by analyzing their community structure. The detection of communities of pores, defined as densely connected groups with only sparser connections between them, contributes to the characterization of porous media and may help us to better understand the diffusion of gas and water, the biodiversity, and other complex phenomena in soils.

The article is presented as follows. In the next section, we describe the characteristics of the four porous soil samples as well as the model we used. In the third section, we describe the two algorithms we used to detect communities in the networks. In the fourth section, we present the results of both algorithms applied to the four soil samples. In the last section, we present our conclusions.

POROUS SOIL MODEL

The structure of a porous soil is modeled as a heterogeneous complex network, where nodes v_i correspond to pores and links e_{ij} correspond to fluid flows between the pores associated to nodes v_i and v_j. The upper plot of Fig. 1 illustrates the network representation of a soil sample. The links will be considered undirected $e_{ij} = e_{ji}$ and thus the connectivity degree k_i of a node v_i will be a measure of the number of pores directly connected with the associated pore. The properties of a pore v_i are described by the node state (r_i, s_i), which account for the position r_i of the pore center in the soil and the pore size s_i.

The evolution of the porous soil structure is modeled as a stochastic growth process described by HPA (Santiago and Benito, 2007a). In the HPA model, the process starts with a seed of arbitrary size and topology. A new node v_a is added to the network at each step, bringing a fixed number m of links attached. These links are preferentially connected to the already existing nodes following the so-called attachment rule: the linking

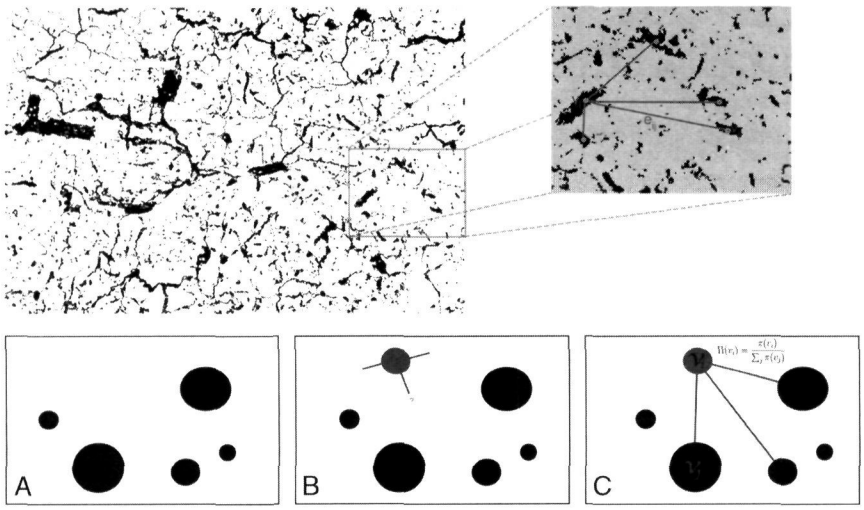

FIG. 1. Upper plot: Soil pore network example corresponding to a subarea of soil image (box). Red lines correspond to links between pores. Lower plots: Representation of the model process. A, Porous system composed of five pores. B, A new pore (red) (with a fixed number m of links attached) is added to the network. C, The m links attached are randomly connected to the network pores following the $\pi(v_i)$ probability function.

probability of a network node v_i is proportional to its degree k_i and the affinity $\sigma\{x_i, x_a\}$ of the node state x_i with the newly added node (see the lower plots of Fig. 1). This step is iterated until a desired number of nodes have been added to the network.

The affinity function σ incorporates the influence of node attributes to the attachment rule, biasing the degree so that higher affinity values yield higher linking probabilities. In the porous soil case, the likelihood that a newly created pore will connect to an existing pore is proportional to the size of the existing pore and inversely proportional to the distance between the pores. Likewise, the larger the number of connections associated with an existing pore, the greater the likelihood that a new flow of fluids will intercept an existing connection and connect the new pore to the older one. Thus, the affinity function $\sigma\{x_i, x_a\}$ of an existing network node v_i when a new node v_a is added will be a monotonous function of s_i and d^{-1} (r_i, r_i), where d is the Euclidean distance.

The previous considerations prompt us to model the dynamics of the porous structure of soils as an HPA model defined by a state space R, a probability distribution $\rho(x)$ of the node states or the intrinsic pore properties considered in the model (size and position), and an affinity function $\sigma(x, y)$ of the interactions between the network nodes. This formalism prescribes the evolution of a network according to the following rules:

1) The nodes v_i are characterized by their state $x_i \in R$ deemed constant in the timescale of evolution of the network.
2) The growth process starts with a seed composed by N_0 nodes (with arbitrary states $x_i \in R$) and L_0 links.
3) A new node v_a (with a fixed number m_0 of links attached) is added to the network at each iteration. The newly added node is randomly assigned a state x_a (size and position) following the distribution $\rho(x)$.
4) The m_0 links attached to v_a are randomly connected to the network nodes following a probability function $\Pi(v_i)$ given by an extended attachment rule:

$$\Pi(v_i) = \frac{\pi(v_i)}{\sum_j \pi(v_j)} \quad , \quad \pi(v_i) = k_i\, \sigma(x_i, x_a) \tag{1}$$

The visibility π of a node v_i is thus given by the product of its degree k_i and its affinity σ with the newly added node v_a, which is itself a function of the states x_i and x_a. Steps 3 and 4 are iterated until a desired number of nodes N have been added to the network. To sum up, the choice of R, ρ, and σ determines the form of heterogeneity in the attachment mechanism.

Consistent with the previous formalism, we define the porous soil model by a state space $R = M \times S$, where M is a Euclidean box with dimension 2 or 3 that represents the medium geometry, and S represents the range of possible pore sizes; a state distribution $\rho(x) = \rho(r, s)$ that represents the probability for a new pore having a certain position r and size s (defined as the area measured in number of pixels belonging to the pore); and an affinity function $(\sigma(x, y))$:

$$\sigma(x, y) = \frac{s_x^a}{(\delta + |r_x - r_y|)^\beta} \tag{2}$$

where δ is a small nonnegative offset that ensures the continuity of σ on the space R^2, while α and β are free parameters that measure the relative importance of the pore size and distance, respectively, in the affinity of the attachment mechanism. For the same size (s_x) and distance $(r_x - r_y)$, higher is α the $\sigma(x, y)$ increases with increasing α and decreases with increasing β.

We define the porosity of the medium (p) as the fraction of void space in the material:

$$p = s_y / s_t \tag{3}$$

where s_y is the sum of all the pores area and s_t is the total area of the modeled soil sample.

The desired number of nodes N that ends the growth process is the least number that yields the porosity of the simulated soil $p > p_0$ for a certain threshold p_0, which is the porosity of the sample medium (as estimated from the soil scans).

Model Application

We used the model to simulate four soil samples selected for their contrasting soil structures and textures (Table 1). The chosen samples show a wide range for the percentages of sand (1.4%–54.0%), silt (15.0%–66.2%), and clay (25.1%–58.0%). Organic matter content was relatively low (0.1%–1.2%) because mainly subsurface horizons were sampled.

Each of the samples was prepared for image analysis following the procedure described by Protz and VandenBygaart

TABLE 1. Texture of soil samples, as measured by the percentages of organic matter, sand, silt, and clay

Soil	Texture	Organic Matter, %	Sand, %	Silt, %	Clay, %
Inter	Silt loam	0.4	3.1	66.2	25.1
Kampong	Clay	1.2	20.0	22.0	58.0
Buso	Sandy clay loam	0.1	54.0	15.0	31.0
Ads	Silt clay loam	1.1	1.4	65.2	33.4

(1998). These sample soils were kindly provided by the University of Guelph, Department of Land Resource Science. For further information about image acquisition and soil properties, we refer the reader to the Canadian Soil Thin Section Collection Web site at http://gis.lrs.uoguelph.ca/cstsc/. The data were obtained by imaging thin sections with a Kodak 460 RGB camera using transmitted and circularly polarized illumination. The data were cropped from 3,060 × 2,036 pixels to 3,000 × 2,000 pixels. Then EASI/PACE software classified the data and the void bitmap separated (individual pixel size was 18.6 × 18.6 μm). Binary images of the soil samples are shown in Fig. 2.

The frequency distribution of distance between pairs of pore centers was calculated for each soil sample to study the spatial arrangement observed and is shown in Fig. 3. The results evidence that the spatial pore center distribution is reasonably Gaussian over the surfaces for all the soil samples considered in this study, in agreement with previous results (Santiago et al., 2008). Based on this, the model assumes a Gaussian spatial distribution of pore centers. We measured the pore sizes in each of the images and estimated the pore size distribution (PSD) for each soil sample. The PSD, denoted as $F(\text{size})$, is presented in Fig. 4. As can be seen, all the soils display a distribution that follows a power law, $F(\text{size}) \approx \text{size}^{\phi}$, except for extremes values. The values of ϕ range from 1.43 to 1.60 in these four samples, and two of the samples (kampong and ads) have identical values ($\phi = 1.43$). This equality may be explained by the fact that pore

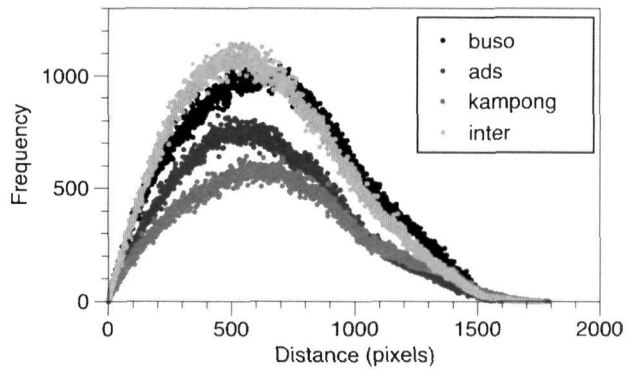

FIG. 3. Frequency distribution of distance between pairs of nodes obtained in the four soil samples.

sizes follow highly non-Gaussian distributions (Perrier et al., 1996), whereas pore positions follow completely Gaussian ones.

The values of the model parameters α and β were chosen according to the following hypothesis. We assume that soils with high percentages of clay and small pore sizes are more compact in comparison with those composed by a high percentage of sand. For this reason, with soils with a higher percentage of clay, the model assigned higher values to the β parameter, giving more weight in the affinity function to the distance between pores (Eq.[2]). On the other hand, we assume that a pore edge in our two-dimensional simulation can be occupied by a higher number of particles in the case of small particles such as clay or silt in comparison with a pore of similar size but generated by large particles such as sand. Thus, the potential pore connectivity in clayey soil is higher than the one in sandy soil. For this reason, α parameter values, associated with the pore area (or size), are lower in sandy soils.

In Table 2, we show the values of α and β chosen according to the soil texture, the value of ϕ obtained from the PSD and the number of pores, maximum size of pores and mean size of pores

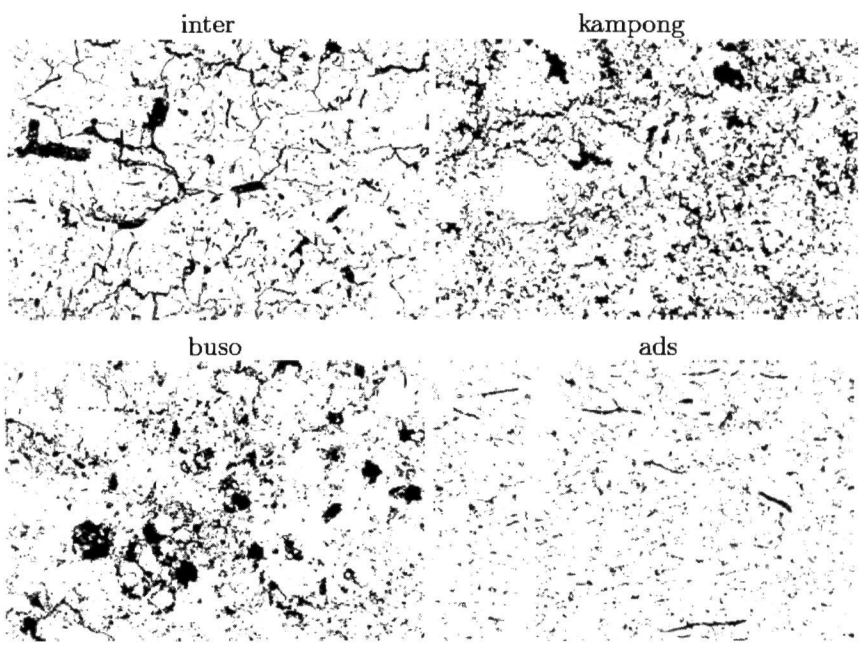

FIG. 2. Binary images of soil samples used in the study. Image sizes are 1,500 × 1,000 pixels. Credit: Richard Heck.

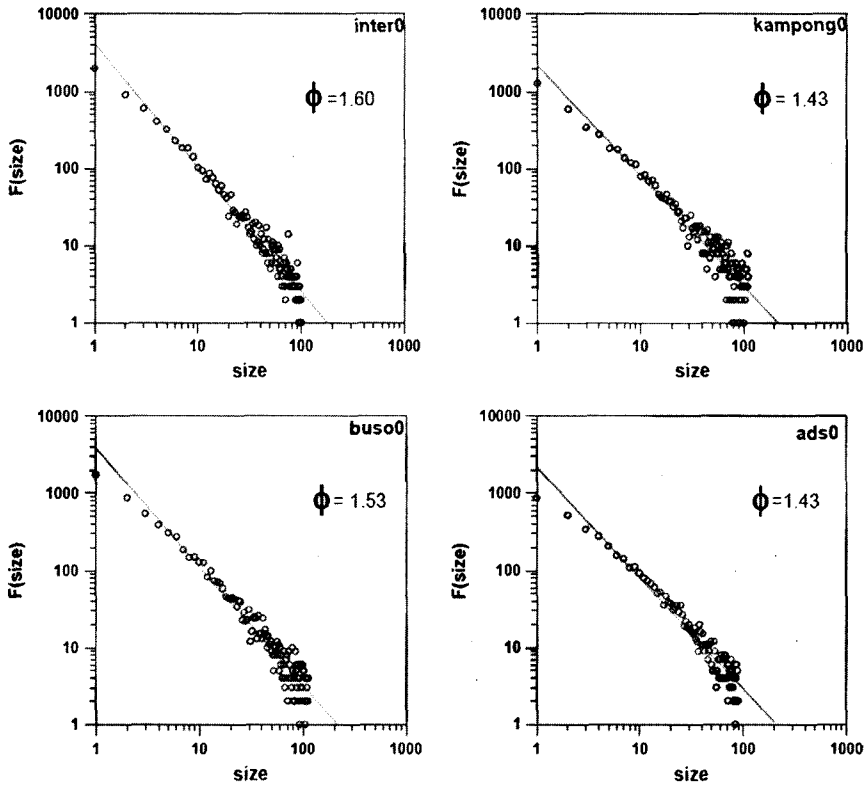

FIG. 4. Pore size distribution, F(size), for soil samples. The value of ϕ corresponds to the scaling exponent of the power law fit denoted by the straight lines. Pore size is measured by the number of pixels.

obtained from each sample. These values were used as data for the model implementation. Table 2 also shows the variance and kurtosis of the PSD. The value of the second statistical moment (σ^2) describes how far the pore sizes disperse from the mean size. The kampong and buso soil samples have a large dispersion of the pore size compared to the inter and ads samples. The high values of the kurtosis, in all the samples, indicate strongly leptokurtic distributions where small sizes of pores are more frequent than the mean size (Fig. 2). This value is again lowest for the ads sample.

Model Results

We analyzed the degree k distribution, which measures the frequency of number of connections of nodes, in each one of the networks generated by the model. In other words, the degree distribution P(k) of a network measures the probability of finding a node with connectivity degree k in the network. Alternatively, the product NP(k) measures the average number of nodes in the network with a given connectivity degree k (Santiago and Benito, 2007b). Figure 5 shows the degree k histograms. As can be seen, all the distributions follow reasonably a power law denoted by the scaling exponent γ. The slight discrepancy between the points of the simulated network and the linear fit, at bi-log scale, at larger degrees (k) is a finite-size effect caused by the limited number of nodes in the simulated networks (Dorogovtsev et al., 2000).

This scaling exponent γ varies from 2.24 (kampong sample) to 2.58 (ads sample), thus not showing a large numerical difference; however, we should take into account that it is the exponent of a power law. For the cases with $\alpha = 0.5$ and $\beta = 2.0$ (inter and ads samples), the degree distribution presents a k maximum range of about 1,000 (Fig. 5). In the case of buso, where β is equal to 1, this maximum is about 4,000. Last, kampong, the only case with $\alpha = 1$, shows a strong nonlinear trend in the bi-log plot degree distribution at less connected pores. Although these results do not reflect the geometrical variety of

TABLE 2. Corresponding parameters α and β used in the model implementation and scaling exponent ϕ of distribution of pore size observed in the samples

Soil	α	β	ϕ	No. Pores	Maximum Size	Mean	σ^2	Kurt
Inter	0.5	2.0	1.60	6,435	100	8.78	96,949.76	1,179.63
Kampong	1.0	2.0	1.43	4,634	110	12.12	120,589.78	250.19
Buso	0.5	1.0	1.53	6,431	114	10.93	223,258.88	2,666.29
Ads	0.5	2.0	1.43	4,113	90	11.68	5,176.60	286.38

For each soil sample, the number of pores, maximum size of pores in pixels (Maximum Size), mean, variance (σ^2), and Kurtosis (Kurt) of the pore size distributions are presented.

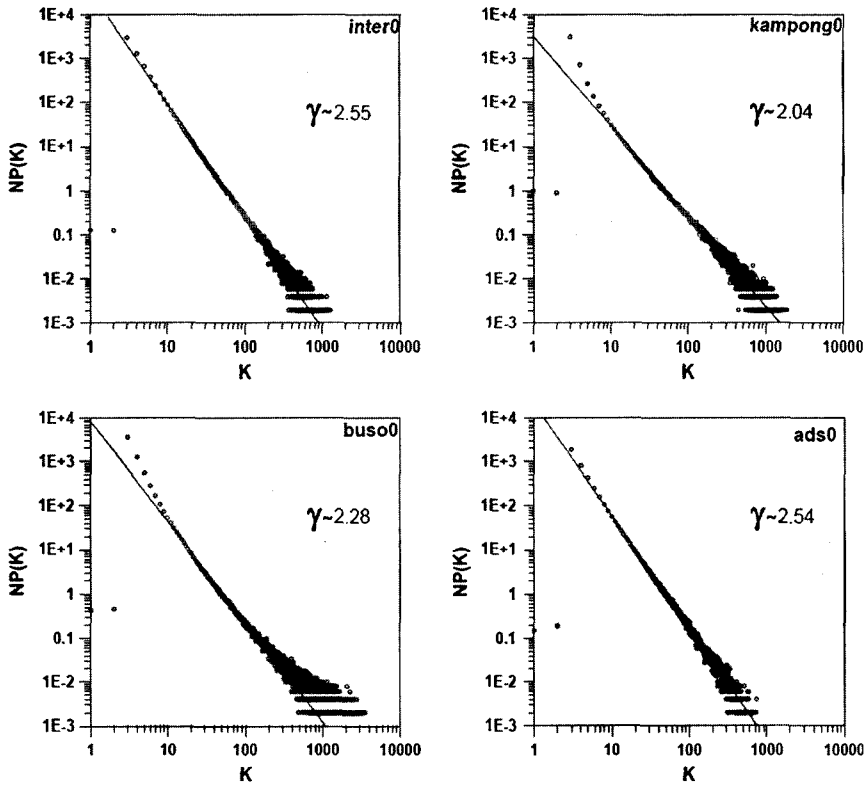

FIG. 5. Distribution of the number of nodes with degree k, $N \times P(k)$, for the soil samples. The value of γ corresponds to the scaling exponent of the fit to a power law.

images shown in Fig. 2, they offer us information about the topology of these pore networks.

Looking with more attention to the soil image corresponding to ads (Fig. 2), the longitudinal pores are clearly predominant though in the case of inter is less obvious. Between these cracks, very small pores are located.

Although links between the nodes in these complex networks do not reflect the true physical connections between pores, they characterize soil structure (Mooney and Korošak, 2009). Therefore, α and β parameters are useful to relate network links with soil texture that have a huge influence in soil porosity and connectivity.

COMMUNITY STRUCTURE OF PORE NETWORKS

Community structure methods normally assume that the network under study is divided naturally into subgroups or communities. The number and size of these communities are determined by the network itself and not by us. In fact, the community structure is a property of the network. For this reason, community structure methods may explicitly admit the possibility that no good division of the network exists.

The central idea of this work is to determine whether there exists any natural division of its pores into nonoverlapping groups or communities, where these communities may be of any size.

Modularity of Pore Networks

The method proposed by Newman (2006) assumes that the N pores that compose the network have a particular division, for example, two groups. Some pores belong to group A and others to group B. Consider $g_i = 1$ if pore v_i belongs to group A and $g_i = -1$ if it belongs to group B. And let a_{ij} be the presence of the link between pores v_i and v_j, the corresponding element of the adjacency matrix, which will be 0 or 1 in our soil porous model.

At the same time, the expected number of edges between pores v_i and v_j if edges are placed at random is $k_i k_j/2m$, where k_i and k_j are the degrees of the pores and $m = 1/2\ \Sigma_i\ k_i$ is the total number of edges in the network. Thus, the modularity, Q, can be written as

$$Q = \frac{1}{4m}\sum_{ij}\left(a_{ij} - \frac{k_i k_j}{2m}\right)(g_i g_j + 1) = \frac{1}{4m}\sum_{ij}\left(a_{ij} - \frac{k_i k_j}{2m}\right)g_i g_j \quad (4)$$

where g is the vector whose elements are the g_i. The leading factor of 1/4m is merely conventional. For more details, see Newman and Girvan (2004).

The method described can be implemented in networks that contain more than two groups or communities. The standard approach to this problem, and the one adopted here, repeats the division into two: the algorithm is used first to divide the network into two parts, then divide those parts, and so forth.

This method proposed by Newman is an optimization task that searches for the maximal value of modularity Q over possible divisions of a network. Thus, the modularity Q obtained corresponds to the best division detected. However, this division may not indicate the presence of communities really. For this reason, we compared the value obtained in each case with the value Q obtained in a model that does not consider any link preference, that is, a pore network in which the pores are randomly linked. These null models correspond to a set of networks generated with the same number of pores and the same distribution of the number of links per pore, the well-known degree distribution P(k). Table 3 shows the modularity Q for the four

soil samples previously described compared with their random null models.

As can be seen, the networks that represent inter and kampong soils display community structure compared with their null models. However, soils such as buso and ads do not have a strong community structure.

The value of Q describes the whole network in terms of its internal structure. With the aim of understanding the results, we applied the algorithm of fast modularity optimization by Blondel et al. (2008) and Lancichinetti and Fortunato (2009) to make a partition of pores into communities and relate the modularity and partition to the parameters of the porous soil model.

Community Partition in Pore Networks

The algorithm proposed by Blondel et al. (2008) is a multistep technique based on a local optimization of the Newman-Girvan modularity (Q) (Newman and Girvan, 2004) in the neighborhood of each node. The method consists of two phases. First, the algorithm looks for small communities by optimizing modularity in a local way. Second, it aggregates nodes of the same community and builds a new network with such communities collapsed into single supernodes. These steps are iterated until a maximum of modularity is attained.

The output of the method therefore gives several partitions. The partition found after the first step typically consists of many communities of small sizes. At subsequent steps, larger and larger communities are found because of the aggregation mechanism. This process naturally leads to hierarchical decomposition of the network.

Figure 6 shows the resulting partition of pores after five steps of the Blondel algorithm. Nodes are represented as spheres located in the space with different sizes (both pore properties, size and location, were generated by the porous soil model). All the pores are colored according to the community to which they belong; thus, pores with the same color belong to the same community.

The networks corresponding to inter and kampong samples show that pores are clearly clustered into spatial communities, that is, spheres of the same color are located very closely to one another. These soils are the same ones that obtain a high Q value in the previous analysis. On the contrary, samples with a low modularity Q, such as buso and ads, do not evidence a clear spatial structure of communities.

Both kampong and ads samples have a low value of ϕ (Fig. 4). The parameter α is 1 for kampong and 0.5 for ads (Table 2), and the difference in Q value is significant (Table 3). In the case of ads, the α value has diminished the influence of PSD in the links resulting in the highest value of γ (Fig. 5). The inter and buso soils have larger values of ϕ, and β values of 2 for inter and 1 for buso; the distance between pores has less influence on their linking probability for the buso soil because the β parameter is smaller. However, the differences in γ are smaller than those in the first comparison. This can be explained by the similar spatial distribution of the pore centers in all the four soil samples, which is influenced by β (see Eq.[2]).

TABLE 3. Modularity Q for the networks generated by the porous soil model for the soil samples under study in comparison with the ones generated with a random network model Q_r[†]

Soil	Q	Q_r
Inter	0.47	0.37 ± 0.01
Kampong	0.43	0.35 ± 0.01
Buso	0.35	0.34 ± 0.01
Ads	0.38	0.35 ± 0.02

[†]An average of a set of 10 networks without preferential attachment with the same size and same degree distribution for each case.

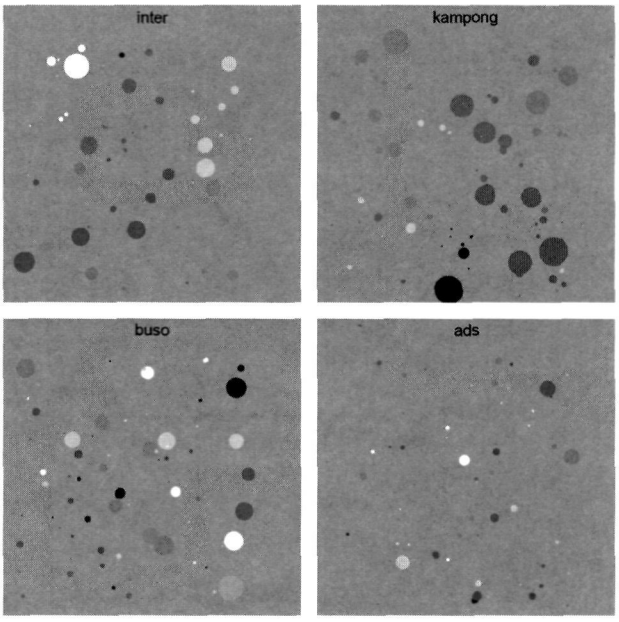

FIG. 6. Community structure of the networks generated by the porous soil model. Each one represents the four soil samples under study. The color indicates the community to which pores belong. The diameter and the spatial position of the pores were generated by the model in boxes of 1,000 × 1,000 pixels. Notice that the links between pores are not represented.

Considering the results, we can conclude that the PSD and the free parameters used in the model determine the community structure of the pore networks. For soils simulated with remarkably inhomogeneous PSD, such as inter and buso, we expected highly connected pores. Despite the presence of highly connected pores, communities are not guaranteed. However, inhomogeneous PSD and high values of β allow the formation of spatial communities around big pores, as seen in the inter and kampong networks in Fig. 6. The contrary occurs in the buso network, where the distance between pores is less important ($\beta = 1$), despite being a network built with an inhomogeneous PSD. The case of ads is interesting, despite having a high value of $\beta = 2$, they do not show a community structure. In this case, the effect of α is strong because of a more homogeneous PSD distribution (Table 2), as can be seen in its network representation in Fig. 6. A homogeneous porous medium with a small α value allows the model to link pores without the effect of their sizes decreasing the probability of spatial clusters of pores.

CONCLUSIONS

In this article, we have reviewed a complex network model based on an HPA scheme to quantify the structure of porous soils. The analytical solutions for the degree densities and degree distribution of the pore networks generated by the model point out the relationship between the variability in the scaling exponents and the parameters regulating the affinity function, as well as the inhomogeneity of the distributions of pore properties and the consequences of this on the asymptotic behavior of the degree distribution. In particular, it is worth emphasizing that

these networks exhibit a multiscaling of their degree densities according to power laws and that such phenomenon leaves a signature of heterogeneity in the topology of pore networks that can be empirically tested in real soil samples.

We have gone further in this work by studying the community structure of pore networks generated by the soil porous model. We have applied two related methods, first, to characterize the modularity of the networks and, second, to partition the nodes according to communities.

The first method, proposed by Newman, is an optimization algorithm that searches for the maximal value of the quantity known as modularity over possible divisions of a network. The second method corresponds to an iterative algorithm that groups communities (identified by optimizing the modularity of the network) into supernodes generating a new network as a seed for the next iteration.

We observed that the same soils that display a high modularity Q can be well divided into spatial communities according to the Blondel et al. (2008) algorithm. On the contrary, nonclustered spatial networks have a low value of modularity Q.

The presence of communities in the networks generated by the porous soil model depends on the PSD and free parameters of the model. In fact, when the value of β is large, that is, when the distance between pores has strong influence on their linking probability, communities appear in networks simulated with inhomogeneous PSD. If the value of β is low, communities are not formed, even if the soil has been constructed with an inhomogeneous PSD. We also observed that the effect of α in the formation of communities is negligible with inhomogeneous PSD. However, its effect can be strong in soils where most pores are of similar size.

The effect of pore communities on the physical, chemical, and biological properties of soils is strong. In fact, groups of densely connected pores could affect the conditions for crop and microorganisms development. Moreover, these communities may affect the soil aeration, sequestration or emission of greenhouse gases, and volatilization of volatile organic chemicals. We will explore some of these phenomena in future works using dynamic models operating on the networks generated.

ACKNOWLEDGMENTS

This work has been supported by the Spanish MEC under projects no. AGL2010-21501/AGR, no. MTM2009-14621, and i-MATH CSD2006-32. The authors thank Prof. Richard Heck from the Department of Soils and Landscape Processes of Guelph University for the images provided for this work.

REFERENCES

Ball, B. C., C. A. Watson, and J. A. Baddeley. 2007. Soil physical fertility, soil structure and rooting conditions after ploughing organically managed grass/clover swards. Soil Use Manage. 23:20–27.

Barabási, A. L., and R. Albert. 1999. Emergence of scaling in random networks. Science 286:509–512.

Bird, N., M. Cruz Díaz, A. Saa, and A. M. Tarquis. 2006. Fractal and multifractal analysis of pore-scale images of soil. J. Hydrol. 322:211–219.

Blondel, V. D., J. -L. Guillaume, R. Lambiotte, and E. Lefebvre. 2008. Fast unfolding of community hierarchies in large networks. J. Stat. Mech. P10008.

Cárdenas, J. P., A. Santiago, A. M. Tarquis, J. C. Losada, F. Borondo, and R. M. Benito. 2010. Soil porous system as heterogeneous complex network. Geoderma 160:13–21.

Dorogovtsev, S. N., J. F. F. Mendes, and A. N. Samukhin. 2000. Structure of growing networks with preferential linking. Phys. Rev. Lett. 85: 4633–4636.

Lancichinetti, A., and S. Fortunato. 2009. Community detection algorithms: A comparative analysis. Phys. Rev. E. 80:056117.

Leij, F. J., T. A. Ghezzehei, and D. Or. 2002. Analytical models for soil pore-size distribution after tillage. Soil Sci. Soc. Am. J. 66:1104–1114.

Mooney, S. J., and D. Korošak. 2009. Using complex networks to model two- and three dimensional soil porous architecture. Soil Sci. Soc. Am. J. 73:1094–1100.

Newman, E. J. 2006. Modularity and community structure in networks. Proc Natl Acad Sci USA 103(23):8573–8574.

Newman, M. E. J., and M. Girvan. 2004. Finding and evaluating community structure in networks. Phys. Rev. E. 69:026113.

Perrier, E., M. Rieu, G. Sposito, and G. de Marsily. 1996. Models of the water retention curve for soils with a fractal pore size distribution. Water Resour. Res. 32:3025–3031.

Protz, R., and A. J. VandenBygaart. 1998. Toward systematic image analysis in the study of soil micromorphology. Sci. Soils 3:34–44.

Santiago, A., and R. M. Benito. 2007a. Emergence of multiscaling in heterogeneous complex networks. Int. J. Mod. Phys. C. 18:1–17.

Santiago, A., and R. M. Benito. 2007b. Connectivity degrees in the threshold preferential attachment model. Physica A. 387:2365–2376.

Santiago, A., and R. M. Benito. 2008. An extended formalism for preferential attachment in heterogeneous complex networks. Europhys. Lett. 82:58004.

Santiago, A., and R. M. Benito. 2009. Improved clustering through heterogeneity in preferential attachment networks. Int. J. Bifurc. Chaos 19(3):1029–1036.

Santiago, A., J. P. Cárdenas, J. C. Losada, R. M. Benito, A. M. Tarquis, and F. Borondo. 2008. Multiscaling of soils as heterogeneous complex networks. Nonlinear Proc. Geophys. 15:893–902.

Tarquis, A. M., R. J. Heck, D. Andina, A. Alvarez, and J. M. Antón. 2009. Pore network complexity and thresholding of 3D soil images. Ecol. Complex. 6:230–239.

VandenBygaart, A. J., R. Protz, and A. D. Tomlin. 1999. Changes in pore structure in a no-till chronosequence of silt loam soils, southern Ontario. Can. J. Soil Sci. 79:149–160.